

Attenuation of transverse ultrasonic waves near the diffuse solid electrolyte transition in CdF₂

M. O. Manasreh* and D. O. Pederson

Department of Physics, University of Arkansas, Fayetteville, Arkansas 72701

(Received 9 October 1984)

The attenuation of transverse ultrasonic waves propagating approximately in the [111] direction in CdF₂ has been studied as a function of temperature from 300 to 1060 K and frequency from 8 to 19 MHz. The ultrasonic attenuation peaks observed have been used to define a diffuse transition temperature in CdF₂ of 981 K, which is well below the melting temperature of 1373 K. The ultrasonic attenuation coefficient was determined to be proportional to the square of frequency over the entire range of temperature. The Arrhenius energy of anion motion above 981 K was obtained from the temperature dependence of the attenuation and the theory of local site fluctuations.

INTRODUCTION

Divalent-metal halides of the fluorite structure comprise one class of materials variously known as solid electrolytes, fast-ion conductors, or superionic conductors. The conductivity in these materials which is a result of halide motion is characterized by Arrhenius behavior up to a diffuse transition with negative deviations from Arrhenius behavior or conductivity saturation above the transition. Anionic conductivities as high as $4 (\Omega \text{ cm})^{-1}$ in PbF₂ are typical of the high-temperature conductivity in these materials.^{1,2} The diffuse transition is characterized by a broad heat-capacity peak³⁻⁵ over a range of temperatures around T_c accompanied by a lattice softening,⁶⁻⁸ both of which are indicative of the development of relatively high disorder in the anion sublattice.⁹ The anion disorder well below T_c is associated principally with the thermally-induced defect identified as an anion Frenkel pair consisting of an interstitial anion close to the center of one of the empty cubes in the fluorite structure and an associate anion vacancy.¹⁰ There is considerable evidence now that the defects, particularly near and above T_c , are more complicated than an isolated anion Frenkel pair.¹¹ Nevertheless, the fluorite materials are structurally simpler than other classes of solid electrolytes and therefore are more amenable to understanding high ionic conductivity in solids. The present work on CdF₂ reports on the frequency and temperature dependence of transverse ultrasonic attenuation. Previous longitudinal ultrasonic measurements¹² in CdF₂ have demonstrated that CdF₂ is similar to other fluorites with $T_c = 983$ K.

THEORY

The phenomenon of interest in the present work is the interaction of long-wavelength phonons with the mobile anions in the fluorite lattice. Huberman and Martin¹³ have given a theory of the dynamics of the coupled crystalline-cage charged-liquid fluctuations in superionic conductors which takes into account both local and nonlocal excitations of the system. Such a coupling can be visualized as an effective-frequency and wave-vector-dependent modulation of the chemical potential felt by

the mobile ions. This theory predicts that fluctuations in local-site populations dominate the charged-density fluctuations. The local-site fluctuations couple to pure volume strains or pure shear strains where ions are redistributed among energetically inequivalent or equivalent sites, respectively. For the weak coupling and low-frequency limit, Huberman and Martin's result for ultrasonic attenuation can be written as

$$\alpha = \omega_k^2 T_c [(\rho/C)^{1/2}/R(T)T], \quad (1)$$

where ρ is the material's mass density, C is the elastic constant, ω_k is the angular frequency of the propagating acoustic wave, T_c is the diffuse transition temperature, and T is the temperature. The relaxation rate or frequency $R(T)$ reflects the coupling of the pseudospin, which describes the local degrees of freedom of site occupation to the thermal reservoir provided by the crystalline cage, and in general has an Arrhenius behavior,

$$R(T) = 1/\tau = R_0(T) \exp(-E/kT), \quad (2)$$

where τ is the relaxation time, $R_0(T)$ is the relaxation-attempt rate or frequency, expected to be of the order of an optical-phonon frequency (10^{12} to 10^{13} Hz), and E is the activation energy for the hopping of mobile ions between available sites.

EXPERIMENT

Three 0.62-cm-long crystals were cut from a 4-cm-long and 1-cm-diam crystal of CdF₂ obtained from Optovac, Inc.¹⁴ The crystal axis was determined by back-reflection Laue photography to be oriented 11° from the [111] direction. The end faces of each sample were polished parallel to within four parts in 10^4 .

The electronic equipment generally has been described elsewhere¹⁵ with the attenuation measured by a switchable attenuator inserted in the rf-signal line to the oscilloscope. The du Pont 9770 platinum- and silver-conductor composition has been previously used as an effective acoustic bond at high temperature in divalent metal fluorides for compressional¹⁶ and shear¹⁷ acoustic waves. The transducers used for these transverse ultrasonic attenuation

measurements were nominally 2.5, 10, and 15 MHz, 41° *x*-cut lithium niobate transducers. The 10- and 15-MHz transducers were operated at their loaded fundamental resonant frequencies while the 2.5-MHz transducer was operated at its loaded ninth overtone resonant frequency. The frequency range was limited by the bandwidth of the electronic equipment available. The temperature was measured using a type-K chromel-alumel thermocouple with an Omega-CJ (cold-junction) compensator and Keithley 171 digital multimeter. A Lindberg Hevi-duty furnace was used in this work. The measurements were performed in a vacuum of approximately 4×10^{-3} Pa (3×10^{-5} Torr). An accuracy of ± 0.5 dB in the ultrasonic attenuation measurement could be achieved. This accuracy in the ultrasonic attenuation measurements yields an estimated error of ± 0.10 eV in the activation energy measurements. The precision of the ultrasonic attenuation coefficient is calculated to be ± 0.41 , 0.22, and 0.21 dB/cm from the standard deviation of the data about smoothly increasing functions for 8, 13, and 19 MHz, respectively. The frequency was adjusted slightly during every run to maintain the same pattern of the echoes on the oscilloscope. The variations of frequency were ± 0.3 , ± 0.6 , and ± 0.9 MHz for 8, 13, and 19 MHz, respectively.

RESULTS

In addition to the ultrasonic attenuation due to the interaction of phonons with the mobile ions, the measured attenuation includes crystal nonparallelism, bond and diffraction losses, as well as attenuation due to the interaction of the ultrasonic wave with the thermal phonons. The apparent attenuation due to the nonparallelism of the two ends of the crystal was estimated both by measuring the nonparallelism directly and by measuring the ultrasonic echo-pattern envelope minima.^{18,19} Both estimates were in general agreement and the value obtained from the envelope minima was subtracted from all values of measured attenuation. Even though the du Pont 9770 bonds between the transducer and the sample were generally thin, these bonds were measured to have a higher ultrasonic loss than bonds made of Dow resin 276-V9 which would also transmit shear waves. This additional bond attenuation which must represent a lower bound to the total bond loss was subtracted from all values of measured attenuation. Since an acoustic beam spreads out

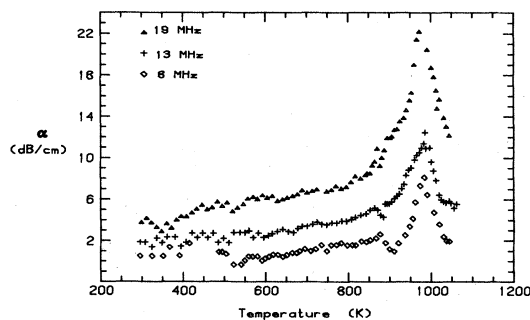


FIG. 1. Temperature dependence of the ultrasonic attenuation coefficient α of CdF_2 measured at 8, 13, and 19 MHz.

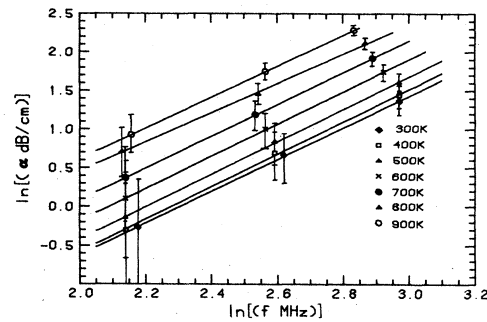


FIG. 2. Frequency dependence of the ultrasonic attenuation coefficient α at different temperatures for CdF_2 using the data of Fig. 1 with the solid lines representing the first-order least-squares fit of the data.

from the transducer's finite size into a diffraction field, the ultrasonic pulse amplitude is modulated and depends on the ratio of the transducer radius squared to acoustic wavelength and on the distance the pulse travels. An expression for the diffraction correction to longitudinal echo attenuation measurements is available.²⁰ In the present work the diffraction correction for the transverse ultrasonic measurements was estimated by utilizing the longitudinal diffraction correction and was subtracted from all values of the measured attenuation. The aforementioned corrections taken together were approximately 2 to 7 dB/cm depending on frequency and, for the nonparallelism correction, on temperature. Ultrasonic attenuation due to acoustic-wave interaction with thermal phonons is independent of temperature²¹⁻²³ at temperatures greater than the Debye temperature which is 332 K for CdF_2 .²⁴ This attenuation depends on the frequency squared as do the present experimental results, but for CdF_2 the calculated ultrasonic attenuation for frequencies less than 20 MHz due to the interaction of the acoustic wave with thermal phonons is much less than other corrections or experimental uncertainties. This calculated attenuation is comparable to that found in alkaline-earth fluorides which is less than 0.01 dB/cm at 20 MHz²⁵ and is therefore negligible in the present measurements. The ultrasonic attenuation coefficient α for 8, 13, and 19 MHz transverse waves, propagating approximately in the [111] direction in CdF_2 , is shown in Fig. 1 as a function of temperature. The result in Fig. 1 shows a large peak at 981

TABLE I. Coefficients of the first-order least-squares fit $\ln \alpha = A + B \ln v$ of the ultrasonic attenuation of CdF_2 at various temperatures with the standard error of the lines presented in Fig. 2.

Temperature (K)	A	B	Standard error
300	-4.746	2.059	0.018
400	-4.787	2.101	0.040
500	-4.641	2.107	0.022
600	-4.375	2.093	0.012
700	-4.054	2.070	0.004
800	-3.344	1.899	0.339
900	-3.411	2.009	0.001

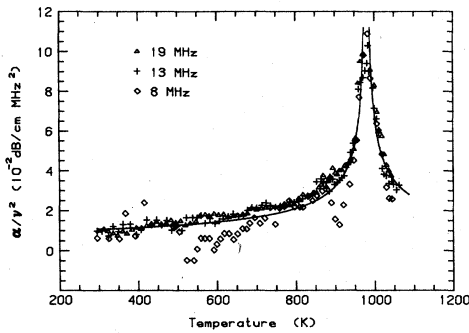


FIG. 3. Temperature dependence of α/v^2 of CdF₂ using the data of Fig. 1 with the solid line representing $\alpha/v^2 = 0.316 |T_c - T|^{-0.521}$.

K. Variations of the ultrasonic attenuation coefficient at different temperatures are given in Fig. 2 as a function of frequency. The ultrasonic attenuation coefficient was derived as a function of frequency from the second-order least-squares fit of the data of Fig. 1 in the temperature range of 300–900 K. The solid lines in Fig. 2 represent the first-order least-squares fit of the data at three different frequencies with the coefficients given in Table I. It is shown from Fig. 2 and Table I that the ultrasonic attenuation coefficient is approximately proportional to the square of the frequency. The temperature dependence of the ultrasonic attenuation coefficient divided by the square of the frequency (α/v^2) is shown in Fig. 3. The data are in agreement over the entire temperature range of 300–1050 K for the three different frequencies. The overlapping of the data in Fig. 3 in the vicinity of the transition temperature agrees with the frequency dependence of Huberman and Martin theory¹³ [see Eq. (1)] in that the ultrasonic attenuation coefficient is proportional to the square of frequency. The solid line in Fig. 3 was determined by a least-squares fit of the data both above and below T_c in the form $\alpha/v^2 = A |T_c - T|^{-B}$ by varying T_c over the range 975–987 K. The minimum standard error was for 981 ± 1 K though the accuracy of the measured temperature in this range is probably not better than ± 10 K. The calculated fit is $\alpha/v^2 = 0.316 |981 - T|^{-0.521}$. The form of the equation is not meant to imply that there is evidence of a true phase transition since the precision of this data is insufficient and only in one run of the three reported here did the signal actually disappear near T_c entirely into the noise.

DISCUSSION

It is clear from Figs. 2 and 3 that there is a temperature dependence which is not characteristic of the usual acoustic-wave interaction with thermal phonons. The transverse ultrasonic attenuation peak centered around 981 K agrees with the longitudinal ultrasonic attenuation peak at 983 K also observed in CdF₂.¹² All of these ultrasonic attenuation peaks have been observed to occur simultaneously with anomalous decreases in the associated

elastic constant. This is evidence that what is being observed is the diffuse transition found in the fluorite solid electrolytes. The exponent found in the fit to the data given in Fig. 3 agrees well with a similar exponent found in CdF₂ for the longitudinal ultrasonic attenuation peak.¹²

The temperature variation of the relaxation rate $R(T)$ of CdF₂ was obtained by analyzing the ultrasonic attenuation measurements above $T_c = 981$ K using Eq. (1). Figure 4 shows the plot of the natural log of $R(T)/R_0(T)$ versus $1/kT$ for the three different frequencies taking $R_0(T)$ to be an optical frequency of 10^{12} Hz. There is evidence in the ionic conductivity data for different Arrhenius activation energies for the hopping of mobile ions between available sites near and above T_c . The highest Arrhenius activation energy measured for a particular fluorite has heretofore been below and up to the temperature T_c with lower values well above T_c .^{2,26,27} There is a clear change in slope for the 13-MHz data in Fig. 4 at 1033 K which is not observed clearly for the 8-MHz data or at all for the 19-MHz data, neither of which included the high temperatures obtained at 13 MHz. The solid line for temperatures below 1033 K in Fig. 4 is the first-order least-squares fit of the data for all three frequencies. The limit of 1033 K is determined by the apparent change in slope observed for the 13-MHz data. The solid line shown in Fig. 4 above 1033 K is the first-order least-squares fit of only the 13-MHz data. Equation (2) predicts that the slopes of the solid lines in Fig. 4 are the activation energies for the hopping of mobile ions between available sites. The activation energy obtained from Fig. 4 using all three frequencies below 1033 K is 1.86 ± 0.19 eV, in good agreement with the activation energy obtained from the longitudinal acoustic wave.¹² Values of the activation energy that are obtained from transverse and longitudinal acoustic waves agree well within the estimated error. The Arrhenius activation energy obtained from Fig. 4 above 1033 K for the 13-MHz data only is 0.21 ± 0.15 eV. There are no previously measured activation energies above T_c for CdF₂ available²⁷ for comparison. It is clear that these activation energies do not correspond in any simple way to the anion Frenkel pair formation energy or the activation

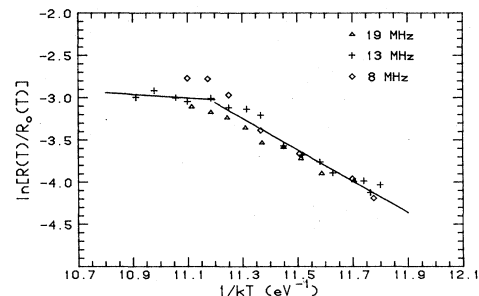


FIG. 4. Experimentally derived values of $R(T)/R_0(T)$ from the ultrasonic attenuation data of Fig. 1 above 981 K with the solid lines representing the first-order least-squares fit of the data at all three frequencies in the range 981–1033 K and of the 13-MHz data in the range 1033–1060 K whose slopes are the Arrhenius activation energies of the anion motion.

energy for vacancy or interstitial motion.² Calculation of the Arrhenius activation energy associated with the defect clusters that explain the neutron scattering data¹¹ is beyond the scope of this present work.

The best previously determined value for the enthalpy of formation of an anion Frenkel defect in CdF₂ of 2.1 ± 0.1 eV²⁸ is from diffusion experiments since it is likely that conductivity measurements have included an electronic contribution due to the high reactivity of CdF₂ at high temperatures.^{27,29} The present ultrasonic measurements like the diffusion measurements are affected less by surface contamination. Although a direct measurement of the anion Frenkel pair formation energy is not available from the ultrasonic attenuation measurements, the observation of T_c provides, through the correlation observed between the temperature T_c and the Frenkel energy E_F , an estimate of the anion Frenkel defect formation energy.³⁰ Utilizing the expression $E_F \approx 20kT_c$, a Frenkel energy for CdF₂ can be estimated to be 1.7 eV. This value agrees with the value from the diffusion experiment within estimated error limits of ± 0.3 eV as determined from the correlation for other fluorites.

CONCLUSION

The present study has provided the new measurements of the transverse ultrasonic attenuation in CdF₂ up to 1060 K. The behavior of the ultrasonic attenuation near 981 K is identical to that observed in the longitudinal ultrasonic measurements in approximately [111] CdF₂ near the diffuse transition. The transverse ultrasonic attenuation peaks, which are used to define the transition temperature of $T_c = 981$ K, are associated only with ion motion rather than in combination with a crystallographic phase transition as in RbAg₄I₅.³¹ The ultrasonic attenuation is approximately proportional to the square of frequency over the entire range of temperature of 300–1060 K.

The Arrhenius activation energies obtained from the temperature dependence of the transverse ultrasonic attenuation due to mobile anions are 1.86 eV in the temperature region between $T_c = 981$ and 1033 K and 0.21 eV in the region between 1033 and 1060 K. Additional work is required to understand the mechanism of anion motion near and above T_c .

*Present address: Department of Electrical Engineering, University of Arkansas, Fayetteville, AR 72701.

¹V. M. Carr, A. V. Chadwick, and R. Saghafian, *J. Phys. C* **11**, L637 (1978).

²A. Azimi, V. M. Carr, A. V. Chadwick, F. G. Kirkwood, and R. Saghafian, *J. Phys. Chem. Solids* **45**, 23 (1984).

³V. R. Belosludov, R. I. Efremova, and E. V. Matizen, *Fiz. Tverd. Tela (Leningrad)* **16**, 1311 (1974) [*Sov. Phys.—Solid State* **16**, 847 (1974)].

⁴W. Schröter, Ph.D. thesis, University of Göttingen, 1979.

⁵W. Schröter and J. Nolting, *J. Phys. (Paris) Colloq.* **41**, C6-20 (1980).

⁶C. R. A. Catlow, J. D. Comins, F. A. Germano, R. T. Harley, and W. Hayes, *J. Phys. C* **11**, 3197 (1978).

⁷M. H. Dickens, W. Hayes, M. T. Hutchings, and W. G. Kleppmann, *J. Phys. C* **12**, 17 (1979).

⁸M. O. Manasreh and D. O. Pederson, *Phys. Rev. B* **30**, 3482 (1984).

⁹W. Hayes, *J. Phys. (Paris) Colloq.* **41**, C6-7 (1980).

¹⁰C. R. A. Catlow, *Comments Solid State Phys.* **9**, 157 (1980).

¹¹M. T. Hutchings, K. Clausen, M. H. Dickens, W. Hayes, J. K. Kjems, P. G. Schnabel, and C. Smith, *J. Phys. C* **17**, 3903 (1984).

¹²M. O. Manasreh and D. O. Pederson, *Solid State Ionics* **15**, 65 (1985).

¹³B. A. Huberman and R. M. Martin, *Phys. Rev. B* **13**, 1498 (1976).

¹⁴Optovac, Inc., North Brookfield, MA 01535.

¹⁵D. O. Pederson and J. A. Brewer, *Phys. Rev. B* **16**, 4546

(1977).

¹⁶R. B. Foster, J. A. Brewer, S. R. Montgomery, and D. O. Pederson, *J. Acoust. Soc. Am.* **73**, 352 (1983).

¹⁷M. O. Manasreh and D. O. Pederson, *J. Acoust. Soc. Am.* **75**, 1766 (1984).

¹⁸R. Truell and W. Oates, *J. Acoust. Soc. Am.* **35**, 1382 (1963).

¹⁹R. Truell, C. Elbaum, and B. B. Chick, *Ultrasonic Methods in Solid State Physics* (Academic, New York, 1969).

²⁰E. P. Papadakis, *J. Acoust. Soc. Am.* **40**, 863 (1966).

²¹A. Akhieser, *J. Phys. (Moscow)* **1**, 277 (1939).

²²H. Bommel and K. Dransfeld, *Phys. Rev.* **117**, 1245 (1960).

²³T. O. Woodruff and H. Ehrenreich, *Phys. Rev.* **123**, 1553 (1961).

²⁴D. O. Pederson, J. A. Brewer, and J. C. Ho, *Phys. Rev. B* **17**, 866 (1978).

²⁵A. D. Gingis, A. I. Morozov, B. A. Stankovskii, and V. V. Golotsvan, *Fiz. Tverd. Tela (Leningrad)* **11**, 2313 (1969) [*Sov. Phys.—Solid State* **11**, 1868 (1970)].

²⁶J. M. Oberschmidt and D. Lazarus, *Phys. Rev. B* **21**, 2952 (1980).

²⁷J. M. Oberschmidt and D. Lazarus, *Phys. Rev. B* **21**, 5823 (1980).

²⁸P. Süptitz, E. Brink, and D. Becker, *Phys. Status Solidi B* **54**, 713 (1972).

²⁹A. Kessler and J. E. Caffyn, *J. Phys. C* **5**, 1134 (1972).

³⁰N. H. March, D. D. Richardson, and M. P. Tosi, *Solid State Commun.* **35**, 903 (1980).

³¹M. Nagao and T. Kaneda, *Phys. Rev. B* **11**, 2711 (1975).